The Astrophysical Journal Letters, 737:L19 (5pp), 2011 August 10 doi:10.1088/2041-8205/737/1/L19

CHANDRA OBSERVATIONS OF A 1.9 kpc SEPARATION DOUBLE X-RAY SOURCE IN A CANDIDATE DUAL ACTIVE GALACTIC NUCLEUS GALAXY AT $z = 0.16$

Julia M. Comerford[1,3], David Pooley[1], Brian F. Gerke[2], and Greg M. Madejski[2]
[1] Astronomy Department, University of Texas at Austin, Austin, TX 78712, USA
[2] Kavli Institute for Particle Astrophysics and Cosmology, M/S 29,
Stanford Linear Accelerator Center, 2575 Sand Hill Road, Menlo Park, CA 94725, USA
Received 2011 June 3; accepted 2011 July 6; published 2011 July 22

ABSTRACT

We report *Chandra* observations of a double X-ray source in the $z = 0.1569$ galaxy SDSS J171544.05+600835.7. The galaxy was initially identified as a dual active galactic nucleus (AGN) candidate based on the double-peaked [O III] λ5007 emission lines, with a line-of-sight velocity separation of 350 km s^{-1}, in its Sloan Digital Sky Survey spectrum. We used the Kast Spectrograph at Lick Observatory to obtain two long-slit spectra of the galaxy at two different position angles, which reveal that the two Type 2 AGN emission components have not only a velocity offset, but also a projected spatial offset of 1.9 h_{70}^{-1} kpc on the sky. *Chandra*/ACIS observations of two X-ray sources with the same spatial offset and orientation as the optical emission suggest that the galaxy most likely contains Compton-thick dual AGNs, although the observations could also be explained by AGN jets. Deeper X-ray observations that reveal Fe K lines, if present, would distinguish between the two scenarios. The observations of a double X-ray source in SDSS J171544.05+600835.7 are a proof of concept for a new, systematic detection method that selects promising dual AGN candidates from ground-based spectroscopy that exhibits both velocity and spatial offsets in the AGN emission features.

Key words: galaxies: active – galaxies: individual (SDSS J171544.05+600835.7) – galaxies: interactions – galaxies: nuclei

Online-only material: color figures

1. INTRODUCTION

A wealth of observations have shown that galaxy mergers are common and that nearly all galaxies host a central supermassive black hole (SMBH). Consequently, some galaxies must host two SMBHs as the result of recent mergers. These are known as dual SMBHs for the first ∼100 Myr after the merger when they are at separations $\gtrsim$1 kpc (Begelman et al. 1980; Milosavljević & Merritt 2001). Dual-SMBH systems are an important testing ground for theories of galaxy formation and evolution. For example, simulations predict that quasar feedback in mergers can have extreme effects on star formation (Springel et al. 2005) and that the core–cusp division in nuclear stellar distributions may be caused by the scouring effects of dual SMBHs (Milosavljević et al. 2002; Lauer et al. 2007). A statistical study of dual SMBHs and their host galaxies would thus have important implications for theories of galaxy formation and SMBH growth.

Dual SMBHs are observable when sufficient gas accretes onto them to power dual active galactic nuclei (AGNs). While there have been identifications of hundreds of binary quasar pairs at separations >10 kpc (e.g., Hennawi et al. 2006; Myers et al. 2007, 2008; Green et al. 2010), as well as a handful of galaxy pairs where each galaxy hosts an AGN (Ballo et al. 2004; Guainazzi et al. 2005; Piconcelli et al. 2010), very few AGN pairs have been observed in the next evolutionary stage where they coexist at kpc-scale separations in the same merger-remnant galaxy. To date, the confirmed dual AGNs were identified by radio or X-ray resolution of two AGNs with separations of 7 kpc in the $z = 0.02$ double radio source 3C 75 at the center of the galaxy cluster A400 (Hudson et al. 2006), 4 kpc in the $z = 0.05$ ultraluminous infrared galaxy Mrk 463 (Bianchi et al. 2008), and 0.7 kpc in the $z = 0.02$ ultraluminous infrared galaxy NGC 6240 (Komossa et al. 2003).

In recent years dual AGN candidates have been selected as galaxies with double-peaked AGN emission lines, first in the DEEP2 Galaxy Redshift Survey (Gerke et al. 2007; Comerford et al. 2009a) and later in the Sloan Digital Sky Survey (SDSS; Wang et al. 2009; Liu et al. 2010b; Smith et al. 2010). Although a double-peaked line profile is expected for dual AGNs, it could also be produced by gas kinematics in a single AGN; follow-up observations are necessary to distinguish between the two scenarios. Follow-up optical long-slit spectroscopy, near-infrared imaging, and adaptive optics imaging have added circumstantial evidence that many double-peaked systems may indeed be dual AGNs (Fu et al. 2011; Liu et al. 2010a; Shen et al. 2011; Greene et al. 2011; Rosario et al. 2011), but direct resolution of two separate AGNs is required for direct evidence of dual AGNs.

Here, we present such evidence for dual AGNs in the form of *Chandra*/ACIS observations of two AGN sources separated by 1.9 h_{70}^{-1} kpc in the $z = 0.1569$ galaxy SDSS J171544.05+600835.7. This galaxy was first identified as a dual AGN candidate by its double-peaked Type 2 AGN spectrum in SDSS, where the [O III] λ5007 peaks are separated by 350 km s^{-1} (Liu et al. 2010b; Smith et al. 2010). Our follow-up Lick/Kast long-slit spectra of the galaxy show two [O III] λ5007 emission components separated on the sky by 1.9 h_{70}^{-1} kpc, or 0.″68, an angular separation resolvable by *Chandra*. The follow-up *Chandra* observations reveal double X-ray sources with the same spatial separation and orientation on the sky as the two [O III] λ5007 emission components, indicating that SDSS J171544.05+600835.7 likely hosts dual AGNs. We assume a Hubble constant $H_0 = 70$ km s^{-1} Mpc^{-1}, $\Omega_m = 0.3$, and

[3] W. J. McDonald Postdoctoral Fellow.

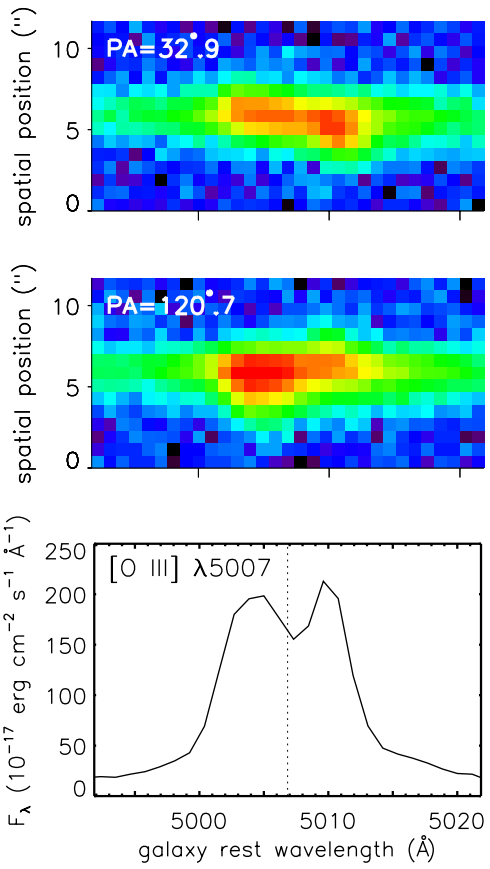

Figure 1. Segments of the two-dimensional Lick/Kast spectra at position angle 32.°9 east of north (top) and position angle 120.°7 east of north (middle), and the SDSS spectrum (bottom) for SDSS J171544.05+600835.7. Each spectrum is shifted to the rest frame of the host galaxy and centered on the rest wavelength of [O III] λ5007 (dotted vertical line). In the Lick/Kast spectra, night-sky emission features have been subtracted and both vertical axes span 11.″7 (31.8 h_{70}^{-1} kpc at the $z = 0.1569$ redshift of the galaxy). The double peaks in [O III] λ5007 in the SDSS spectrum correspond to spatially offset double emission features in the Lick/Kast spectra, suggesting the presence of dual AGNs with a line-of-sight velocity separation of 350 km s^{-1} and a projected spatial separation of 1.9 h_{70}^{-1} kpc (or 0.″68) on the sky. *Chandra* observations support the presence of dual AGNs.

(A color version of this figure is available in the online journal.)

$\Omega_\Lambda = 0.7$ throughout, and all distances are given in physical (not comoving) units.

2. OBSERVATIONS AND ANALYSIS

2.1. SDSS Spectrum

The SDSS spectrum of SDSS J171544.05+600835.7 exhibits several double-peaked Type 2 AGN emission lines, where one peak is blueshifted and one is redshifted relative to the systemic redshift of the host galaxy and the [O III] λ5007 peaks have a line-of-sight velocity separation of 350 km s^{-1} (Liu et al. 2010b; Smith et al. 2010; Figure 1). We fit two Gaussians each to the continuum-subtracted [O III] λ5007, Hβ, [N II] λ6584, and Hα line profiles and used the areas under the best-fit Gaussians as estimates of the line fluxes of the redshifted and blueshifted components of each line. This yields line-flux ratios of [O III] λ5007/Hβ $= 4.4 \pm 1.4$ and [N II] λ6584/Hα $= 1.1 \pm 0.2$ for the blueshifted components, and [O III] λ5007/Hβ $= 8.6 \pm 3.1$ and [N II] λ6584/Hα $= 0.5 \pm 0.1$ for the redshifted components, where the uncertainties are derived from propagating the errors in the parameters of the best-fit Gaussians. These line-flux ratios clearly indicate that both the redshifted and the blueshifted emission components are produced by AGNs (Baldwin et al. 1981; Kewley et al. 2006).

2.2. Lick/Kast Long-slit Spectra

Because spatial information about the double-peaked AGN emission lines can help distinguish whether they are produced by two spatially offset AGNs or gas kinematics from a single AGN, we obtained follow-up slit spectroscopy of the galaxy.

We used the Kast Spectrograph on the Lick 3 m telescope to obtain spectra of the galaxy with a 1200 lines mm^{-1} grating on UT 2009 August 17. To determine the orientation of the AGN emission components on the plane of the sky, we observed the galaxy at two different position angles, 32.°9 east of north and 120.°7 east of north. At each position angle we took three 1200 s exposures, and each spectrum spans the wavelength range 4790–6200 Å. The data were reduced following standard procedures in IRAF and IDL.

The spectra at both position angles reveal two distinct emission components in Hβ, [O III] λ4959, and [O III] λ5007 separated in both velocity and spatial position (Figure 1). The [O III] λ5007 emission has the highest signal-to-noise ratio, which enables the most precise separation measurements. For each spectrum we determine the projected spatial separation between the two [O III] λ5007 emission features by measuring the spatial centroid of each emission component individually, then we combine the projected separation measurements at both position angles to determine the spatial separation and position angle on the sky (for details, see J. M. Comerford et al. 2011, in preparation). We find that the two [O III] λ5007 emission components have a projected separation on the sky of 1.86 ± 0.41 h_{70}^{-1} kpc, or $0.''684 \pm 0.''151$, and the position angle on the sky is 145.°6 east of north.

2.3. Chandra Observations

SDSS J171544.05+600835.7 was observed with the *Chandra X-ray Observatory* on 2011 March 17 beginning at 16:22 UT with an exposure time of 29,669 s. The observation was taken with the telescope aimpoint on the ACIS S3 chip in "timed exposure" mode and telemetered to the ground in "faint" mode. The observation was reduced using the latest *Chandra* software (CIAO 4.3) and the most recent set of calibration files (CALDB 4.4.1). The data were reprocessed with the "chandra_repro" script using the subpixel event repositioning algorithm of Li et al. (2004). Intervals of strong background flaring were searched for, but none were found.

We made a sky image of the field of SDSS J171544.05+600835.7 at a resolution of $0.''0492$ pixel^{-1} (1/10 the size of the physical pixels) with events in the 0.3–8.0 keV energy range, and we fit two-dimensional models to that image. All fits were performed in Sherpa (Freeman et al. 2001) using modified Cash (1979) statistics ("cstat" in Sherpa) and the Nelder & Mead (1965) optimization method ("simplex" in Sherpa). A family of fits was performed, using a grid of parameter starting points to ensure a proper sampling of the multidimensional fit space.

We fit a two-component source model with a fixed background (based on a source-free region near SDSS J171544.05+600835.7). The source model was a β profile, which is a two-dimensional Lorentzian with a varying power law of the form $I(r) = A(1 + (r/r_0)^2)^{-\alpha}$ and is a good match to the *Chandra* point-spread function (PSF). The power-law index α was tied

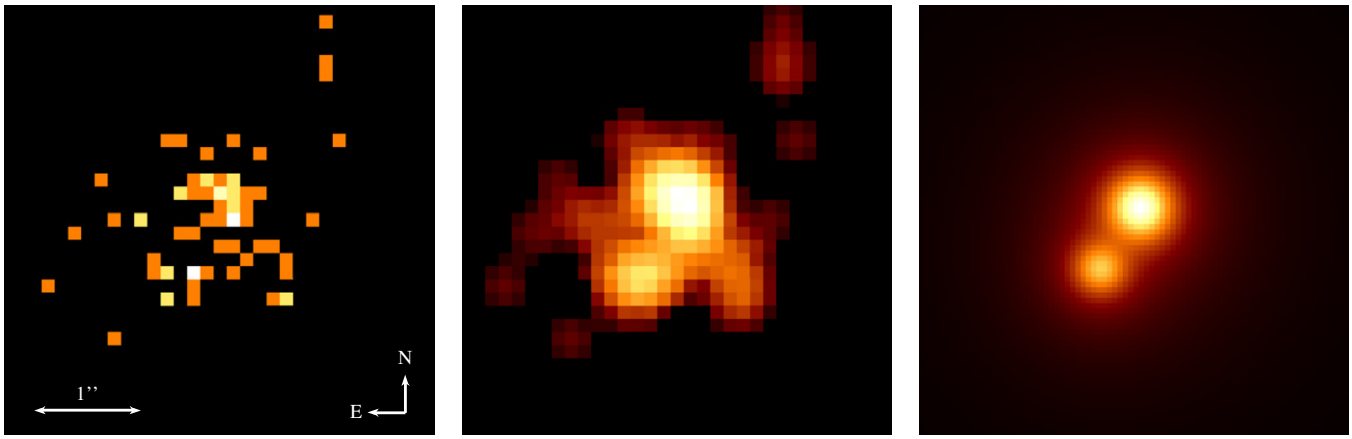

Figure 2. *Chandra* X-ray image of the field of SDSS J171544.05+600835.7 using events in the 0.5–8 keV range (left), data smoothed with a 3 pixel radius Gaussian kernel (center), and image of the two-component β-profile model (right). All images are 4″ on a side.

(A color version of this figure is available in the online journal.)

to the r_0 parameter and both components were required to have the same r_0, which is a model successfully used by Pooley et al. (2009). The components' positions and amplitudes were unconstrained. The best-fit amplitudes are $0.49^{+0.23}_{-0.16}$ and $0.21^{+0.12}_{-0.08}$ counts pixel^{-1} for the northern and southern sources, respectively, and where the southern source is detected at 3.7σ.

The two X-ray components are separated by 1.85 ± 0.22 h_{70}^{-1} kpc, or $0\farcs68 \pm 0\farcs08$, at a position angle of $147^\circ \pm 9^\circ$ east of north, where both the separation and the position angle are consistent with those measured for the two [O III] λ5007 emission components in the Lick/Kast long-slit spectra (Section 2.2). The data, smoothed data, and best-fit model are shown in Figure 2.

To estimate the fluxes of the two components, we cannot reliably extract spectra of and make response files for the two separately. We therefore extracted a spectrum of both sources together and use the results of our two-dimensional image fits to assign appropriate fractions of the total flux to each component. We fit the unbinned spectrum in Sherpa using cstat statistics and the simplex method. The spectral model was a simple absorbed power law with the column density constrained to be at least the Galactic value of $n_H = 2.6 \times 10^{20}$ cm^{-2} (Dickey & Lockman 1990). No additional absorption was preferred in the fit and the best-fit power-law index was 1.9 ± 0.2. The total unabsorbed 0.5–8 keV flux is $(1.5 \pm 0.4) \times 10^{-14}$ erg cm^{-2} s^{-1}. The uncertainty was calculated using the "sample_energy_flux" tool in Sherpa, which takes into account uncertainties in all model parameters. Using the results of our two-dimensional image fit, the northern component has a best-fit flux of $F_{0.5-8} = 1.1 \times 10^{-14}$ erg cm^{-2} s^{-1} and the southern component has $F_{0.5-8} = 4.4 \times 10^{-15}$ erg cm^{-2} s^{-1}.

The 2–10 keV fluxes and absorbed luminosities are $F_{2-10} = (6.4 \pm 3.1) \times 10^{-15}$ erg cm^{-2} s^{-1} ($L_{2-10} = (4.3 \pm 2.1) \times 10^{41}$ erg s^{-1}) for the northern component and $F_{2-10} = (2.7 \pm 1.5) \times 10^{-15}$ erg cm^{-2} s^{-1} ($L_{2-10} = (1.8 \pm 1.0) \times 10^{41}$ erg s^{-1}) for the southern component. We compare the 2–10 keV fluxes to those predicted from the [O III] λ5007 fluxes using the scaling relation for Type 2 AGNs in Heckman et al. (2005), which yields predicted 2–10 keV fluxes of $(3.3 \pm 7.9) \times 10^{-14}$ erg cm^{-2} s^{-1} and $(2.1 \pm 5.1) \times 10^{-14}$ erg cm^{-2} s^{-1} for the redshifted and blueshifted components of [O III] λ5007, respectively. The measured 2–10 keV fluxes are hence a factor of several lower than but within the broad uncertainties of the predictions from Heckman et al. (2005).

Although we cannot fit separate spectra for the two components, we can extract the counts in small regions centered on them and form hardness ratios, defined as HR $= (H - S)/(H + S)$, where H is the number of counts in the 2–8 keV range and S is the number of counts in the 0.5–2 keV range. Counts were extracted from 0.″25 radius regions centered on each source, yielding 20 counts from the northern source with HR $= -0.57^{+0.15}_{-0.19}$ and 10 counts from the southern source with HR $= -0.37^{+0.24}_{-0.30}$. Uncertainties on the hardness ratios were calculated using the Bayesian estimation of hardness ratios package (Park et al. 2006). Judging from the measured hardness ratios, neither source is as hard as would be expected for moderately absorbed (but not Compton-thick) AGNs, although the signal-to-noise ratio is very modest.

2.4. Keck/LGSAO and SDSS Imaging

If SDSS J171544.05+600835.7 has dual AGNs separated by 1.9 h_{70}^{-1} kpc that are the result of a galaxy merger, we might expect the two AGNs to be coincident with two stellar components that are the remnants of the progenitor galaxies in the merger. In fact, SDSS J171544.05+600835.7 was one of 50 SDSS galaxies with double-peaked [O III] lines that was targeted for Keck II laser guide-star adaptive-optics (LGSAO) observations in Fu et al. (2011), which found that 16 of these galaxies exhibited double stellar components with separations 0.6–12 h_{70}^{-1} kpc (or 0.″2–3″), suggestive of merging systems. While Fu et al. (2011) do not show the image of SDSS J171544.05+600835.7, they report that the Keck/LGSAO K'-band image reveals only a single component with $K' = 14.8$ and classify the galaxy as "isolated." The PSF FWHMs for their observations were 0.″065–0.″130, suggesting that SDSS J171544.05+600835.7 may have no substructure at $\gtrsim$0.″1 visible in these K'-band observations.

Based on its SDSS photometry, SDSS J171544.05+600835.7 has a rest-frame $u-r$ color of 2.62 and an absolute r-band magnitude of −22.0, placing it on the red sequence of SDSS galaxies (Baldry et al. 2004). The SDSS image of the galaxy shows no signatures of galaxy interaction (Figure 3).

3. INTERPRETATIONS

Here, we explore the physical mechanisms that could explain the observations of double AGN emission components and X-ray sources in SDSS J171544.05+600835.7.

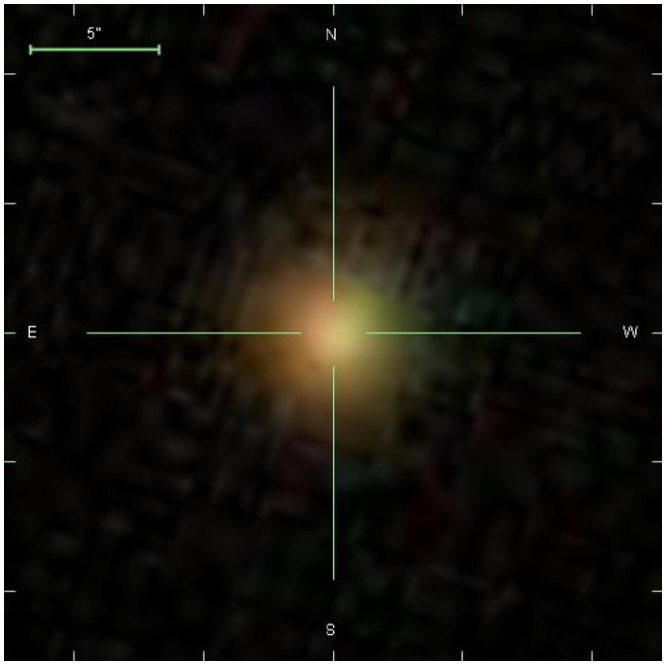

Figure 3. SDSS image of SDSS J171544.05+600835.7. Unlike the dual AGN host galaxies known to date, this galaxy has no indication of extreme star formation or an unusual morphology. This image reveals no tidal features or companions, and no structure on scales $\gtrsim 0\farcs1$ is reported from K'-band adaptive optics imaging (Fu et al. 2011).

(A color version of this figure is available in the online journal.)

The sources' high X-ray luminosities lead us to consider the possibility that they are ultraluminous X-ray sources (ULXs), which are variable off-nuclear X-ray sources. Some ULXs are also candidate intermediate mass black holes (e.g., Kaaret et al. 2003; Farrell et al. 2009). However, estimates of the black hole mass from the optical spectra place SDSS J171544.05+600835.7 in the SMBH regime (Fu et al. 2011). Further, the measured [O III] fluxes and luminosities are well above those typically measured in ULXs (e.g., Porter 2010; Cseh et al. 2011).

Another possibility is that the galaxy hosts dual AGNs that are the result of a triple SMBH interaction, where a gravitational slingshot effect (Saslaw et al. 1974) ejected the least massive SMBH (corresponding to the southern AGN) while the remaining two SMBHs merged (producing the northern AGN). The remaining stellar component associated with the southern AGN could be too faint to appear in the Keck/LGSAO observations. However, the optical observations suggest that both AGNs have associated narrow-line regions and it is unclear how the ejected SMBH would maintain its narrow-line region.

We note also that if there is only a single source visible in the Keck/LGSAO image, a second stellar component could be either obscured or too faint to be within the detection threshold of the Keck/LGSAO observation. If the second stellar component is obscured, the overall extinction for the system still could be skewed toward the low value measured in Section 2.3. Barrows et al. (2011) report a similar case of a dual AGN candidate with a heavily obscured X-ray source and only a single source visible in AO.

Another explanation for our observations is that the galaxy hosts AGN jets that produce both [O III] and X-rays from a combination of photoionization from the AGN and collisional ionization from the jets (e.g., Kraemer et al. 2009; Bianchi et al. 2010). For this scenario to explain our observations, either the AGN is completely obscured and only the jets are visible or one of the sources in our observations is the AGN while the other is the foreground jet and the background jet is obscured or not visible due to de-beaming effects. Both scenarios rely on significant obscuration in part of the galaxy, but this could be consistent with the low column density we measured if the rest of the galaxy is relatively unobscured. However, the jet scenario typically produces a bright core and a much fainter jet, whereas our observations show two sources that differ by only a factor of two in 2–10 keV luminosities.

The observations may also be explained by dual AGNs that are Compton thick. The X-ray spectra alone—if confirmed—exclude Compton-intermediate AGNs, where the absorption would correspond to a column of $\sim 10^{22}$–10^{24} cm^{-2}, as there the observed X-ray flux would be dominated by partially (photoelectrically) absorbed continuum that is detectable as a hard X-ray spectrum. Instead the data suggest that both sources are either unabsorbed or the absorption is severe, essentially resulting in a Compton-thick spectrum. The optical spectra seem to exclude classical, unabsorbed Type 1 AGNs, so we are left with a Compton-thick scenario, with $\tau_{\rm Thomson}$ of at least a few (column $>10^{25}$ cm^{-2}). There, not only the primary nuclear soft X-ray flux is photoelectrically absorbed, but even the hard X-rays are suppressed by Compton opacity, and we detect only primary soft X-rays scattered back to our line of sight, as is the case in, e.g., NGC 1068 and other Compton-thick AGNs. The measured 2–10 keV luminosities for the northern and southern components are within the range of values measured for Compton-thick AGNs (e.g., Levenson et al. 2006). The Compton-thick scenario is also consistent with the low column density of the galaxy, since the column density measurement presupposed that the source was not Compton thick.

We conclude that SDSS J171544.05+600835.7 most likely hosts Compton-thick dual AGNs, because it is the scenario that is most consistent with the existing data. AGN jets might also explain the observations and deeper X-ray observations could distinguish between these two possibilities. These more sensitive X-ray measurements would enable a test of the Compton-thick scenario, since better spectral measurements in the soft X-ray band could provide a possible measurement of the Fe K line, which can have a very high equivalent width in heavily absorbed AGNs but not AGN jets (for a discussion, see, e.g., Levenson et al. 2006; Bassani et al. 1999).

Sensitive hard X-ray measurements would provide much better constraints on the absorbing column. *Hubble Space Telescope* narrowband imaging of the [O III] emission could also show whether it has the biconical morphology expected for AGN jets.

4. CONCLUSIONS

We report observations of a double X-ray source with 1.9 h_{70}^{-1} kpc, or $0\farcs68$, projected spatial separation in the $z = 0.1569$ candidate dual AGN galaxy SDSS J171544.05+600835.7. This Seyfert 2 galaxy exhibits double-peaked [O III] λ5007 emission lines with 350 km s^{-1} line-of-sight velocity separation in its SDSS spectrum and our follow-up Lick/Kast long-slit spectra show two 1.9 h_{70}^{-1} kpc separation [O III] λ5007 emission components. While the velocity and spatial offsets provide circumstantial evidence for dual AGNs, these features could also be produced by gas kinematics from a single AGN. The *Chandra* observations bolster

the evidence for dual AGNs, by revealing two X-ray components suggestive of Compton-thick AGNs with the same spatial separation and orientation as the two sources of optical [O III] λ5007 emission.

To date, dual AGNs have typically been identified serendipitously because of the interesting characteristics of their host galaxies. These host galaxies include ultraluminous infrared galaxies (Komossa et al. 2003; Bianchi et al. 2008), a double radio source at the center of a galaxy cluster (Hudson et al. 2006), and a host galaxy with double bright nuclei and a tidal tail (Comerford et al. 2009b). SDSS J171544.05+600835.7 is unlike these systems because there is nothing particularly noteworthy about the galaxy, which is a seemingly ordinary red-sequence galaxy without tidal features visible in SDSS imaging or substructure reported in adaptive optics imaging. Our observations suggest that dual AGNs may be more ubiquitous and not limited to only galaxies with extreme star formation or unusual morphologies.

We have introduced a systematic, observational method for selecting promising dual AGN candidates, which until now have only been identified through serendipitous discoveries of individual systems. The method consists of three steps: (1) select dual AGN candidates as objects whose spectra exhibit double-peaked AGN emission lines in SDSS or other spectroscopic surveys of galaxies; (2) conduct follow-up long-slit spectroscopy of the dual AGN candidates; and (3) if the follow-up long-slit spectra reveal an object that has two spatially distinct AGN emission components, use follow-up X-ray or radio observations to identify whether the object is a dual AGN system. SDSS J171544.05+600835.7 is the first object for which this technique has been demonstrated and our observations show it most likely hosts dual AGNs; deeper X-ray observations would provide the definitive evidence. Future observations will determine the general applicability of this systematic method for selecting dual AGNs.

J.M.C. acknowledges insightful discussions with Jenny Greene, as well as support from a W.J. McDonald Postdoctoral Fellowship. The Texas Cosmology Center is supported by the College of Natural Sciences and the Department of Astronomy at the University of Texas at Austin and the McDonald Observatory. B.F.G. and G.M.M. were supported by the U.S. Department of Energy under contract number DE-AC02-76SF00515.

REFERENCES

Baldry, I. K., Glazebrook, K., Brinkmann, J., et al. 2004, ApJ, 600, 681
Baldwin, J. A., Phillips, M. M., & Terlevich, R. 1981, PASP, 93, 5
Ballo, L., Braito, V., Della Ceca, R., et al. 2004, ApJ, 600, 634
Barrows, R. S., Stern, D., Madsen, K., et al. 2011, ApJ, submitted
Bassani, L., Dadina, M., Maiolino, R., et al. 1999, ApJS, 121, 473
Begelman, M. C., Blandford, R. D., & Rees, M. J. 1980, Nature, 287, 307
Bianchi, S., Chiaberge, M., Evans, D. A., et al. 2010, MNRAS, 405, 553
Bianchi, S., Chiaberge, M., Piconcelli, E., Guainazzi, M., & Matt, G. 2008, MNRAS, 386, 105
Cash, W. 1979, ApJ, 228, 939
Comerford, J. M., Gerke, B. F., Newman, J. A., et al. 2009a, ApJ, 698, 956
Comerford, J. M., Griffith, R. L., Gerke, B. F., et al. 2009b, ApJ, 702, L82
Cseh, D., Grisé, F., Corbel, S., & Kaaret, P. 2011, ApJ, 728, L5
Dickey, J. M., & Lockman, F. J. 1990, ARA&A, 28, 215
Farrell, S. A., Webb, N. A., Barret, D., Godet, O., & Rodrigues, J. M. 2009, Nature, 460, 73
Freeman, P., Doe, S., & Siemiginowska, A. 2001, Proc. SPIE, 4477, 76
Fu, H., Myers, A. D., Djorgovski, S. G., & Yan, L. 2011, ApJ, 733, 103
Gerke, B. F., Newman, J. A., Lotz, J., et al. 2007, ApJ, 660, L23
Green, P. J., Myers, A. D., Barkhouse, W. A., et al. 2010, ApJ, 710, 1578
Greene, J. E., Zakamska, N. L., Ho, L. C., & Barth, A. J. 2011, ApJ, 732, 9
Guainazzi, M., Piconcelli, E., Jiménez-Bailón, E., & Matt, G. 2005, A&A, 429, L9
Heckman, T. M., Ptak, A., Hornschemeier, A., & Kauffmann, G. 2005, ApJ, 634, 161
Hennawi, J. F., Strauss, M. A., Oguri, M., et al. 2006, AJ, 131, 1
Hudson, D. S., Reiprich, T. H., Clarke, T. E., & Sarazin, C. L. 2006, A&A, 453, 433
Kaaret, P., Corbel, S., Prestwich, A. H., & Zezas, A. 2003, Science, 299, 365
Kewley, L. J., Groves, B., Kauffmann, G., & Heckman, T. 2006, MNRAS, 372, 961
Komossa, S., Burwitz, V., Hasinger, G., et al. 2003, ApJ, 582, L15
Kraemer, S. B., Trippe, M. L., Crenshaw, D. M., et al. 2009, ApJ, 698, 106
Lauer, T. R., Faber, S. M., Richstone, D., et al. 2007, ApJ, 662, 808
Levenson, N. A., Heckman, T. M., Krolik, J. H., Weaver, K. A., & Życki, P. T. 2006, ApJ, 648, 111
Li, J., Kastner, J. H., Prigozhin, G. Y., et al. 2004, ApJ, 610, 1204
Liu, X., Greene, J. E., Shen, Y., & Strauss, M. A. 2010a, ApJ, 715, L30
Liu, X., Shen, Y., Strauss, M. A., & Greene, J. E. 2010b, ApJ, 708, 427
Milosavljević, M., & Merritt, D. 2001, ApJ, 563, 34
Milosavljević, M., Merritt, D., Rest, A., & van den Bosch, F. C. 2002, MNRAS, 331, L51
Myers, A. D., Brunner, R. J., Richards, G. T., et al. 2007, ApJ, 658, 99
Myers, A. D., Richards, G. T., Brunner, R. J., et al. 2008, ApJ, 678, 635
Nelder, J. A., & Mead, R. 1965, Comput. J., 7, 308
Park, T., Kashyap, V. L., Siemiginowska, A., et al. 2006, ApJ, 652, 610
Piconcelli, E., Vignali, C., Bianchi, S., et al. 2010, ApJ, 722, L147
Pooley, D., Rappaport, S., Blackburne, J., et al. 2009, ApJ, 697, 1892
Porter, R. L. 2010, MNRAS, 407, L59
Rosario, D. J., McGurk, R. C., Max, C. E., Shields, G. A., & Smith, K. L. 2011, arXiv:1102.1733
Saslaw, W. C., Valtonen, M. J., & Aarseth, S. J. 1974, ApJ, 190, 253
Shen, Y., Liu, X., Greene, J., & Strauss, M. 2011, ApJ, 735, 48
Smith, K. L., Shields, G. A., Bonning, E. W., et al. 2010, ApJ, 716, 866
Springel, V., Di Matteo, T., & Hernquist, L. 2005, MNRAS, 361, 776
Wang, J., Chen, Y., Hu, C., et al. 2009, ApJ, 705, L76